Semi-active Control of Base Isolation System with Magneto-rheological Fluid Damper

by

Namihiko Inoue[1], Morimasa Watakabe[2], Takafumi Miyama[3], Hidekazu Nishimura[4]

ABSTRACT

To improve a performance of conventional base isolation system, a semi-active MR damper (a variant of oil damper filled with "Magneto-rheological fluid") that can change damping coefficient continuously under magnetic field has been installed into isolation layer. This semi-active base isolated control system is classified into a bilinear system, which an input of the system is proportional to both one of the state vectors and damping factor. To apply a linear control theory like LQR directly, the system has been formed into an equivalent linear system at a certain condition. Since there is some possibility of deterioration of structural performance that is not desirable from the viewpoint of a reduction of acceleration response, we apply the gain-scheduled (GS) control method by transforming the system with the semi-active MR damper to a parameter variation system and finally demonstrate the efficiency of the method successfully.

KEYWORDS: Base Isolation, Gain-scheduled Method, Magneto-rheological (MR) Fluid Damper, Semi-active Control

1. INTRODUCTION

In recent years, there have been many efforts to improve performance of base isolated structures against seismic action. Efficacy of a passive isolated system is well known and the base isolation system consisting of some commercial devices such as LRBs, oil dampers etc. has been applied to many buildings in Japan. Since the passive system is tuned to have specified dynamic property, there are some uncertainties about response under future large earthquakes. To avoid this problem, we take semi-active control that may be more stable and reliable than active control. In this paper we use an MR damper that has same specifications as previously developed one [1][2], which can make damping forces appropriately by input current control. In order to obtain control force we apply a "gain-scheduled" control method. In this method the controller have been calculated appropriately through convex interpolation of some linear time invariant controllers according to certain dynamical systems at vertexes of varying parameters. To apply the GS control, a semi-active damper model with controllable valve is assumed and the system is described as a linear parameter-varying (LPV) model.

2. SYSTEM PARAMETERS

2.1 Specimen

2.1.1 Numerical Model

The experimental setup and numerical model used in this paper are shown in Fig. 1. The specimen has two stories and is settled on a four meters squared, 1-D shaking table in Structural Laboratory of the Building Research Institute that produces an input ground motion by a hydraulic actuator. There are four rubber bearings and four sliding isolators between the shaking table and the first story, and two rubber bearings and two sliding isolators for the second story. To determine the system parameters of this 2DOF system, free vibration tests has been carried out before installing the MR damper. While isolators have been used to avoid twisting motion of masses, some additional friction forces between each story are observed. See Table 1 for detail.

[1] Senior Research Engineer, Department of Structural Engineering, Building Research Institute, Tsukuba-shi, Ibaraki-ken 305-0802 Japan

[2] Research Supervisor, Toda Corporation Research Institute, Tsukuba-shi, Ibaraki-ken 300-2622 Japan

[3] Technical Marketing Engineer, Fujita Corporation Research Center, Atsugi-shi, Kanagawa-ken 243-0125 Japan

[4] Assoc. Professor, Faculty of Engineering, Chiba Univ., Chiba-shi, Chiba-ken 263-8522 Japan

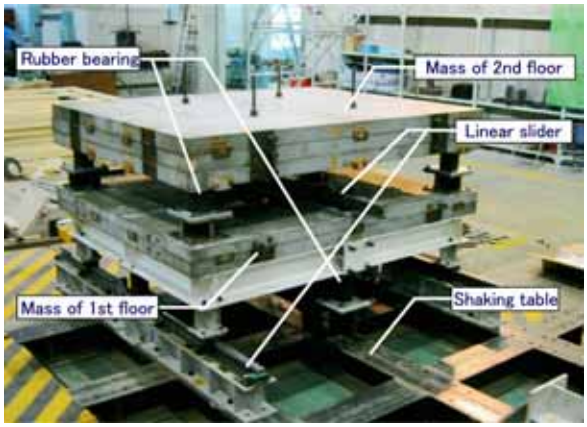

(a) Experimental setup

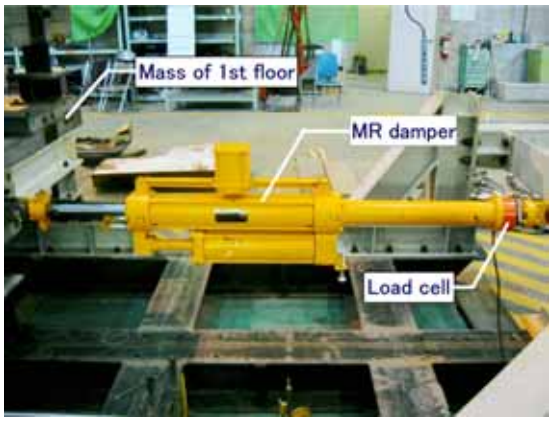

(b) Installation of MR damper

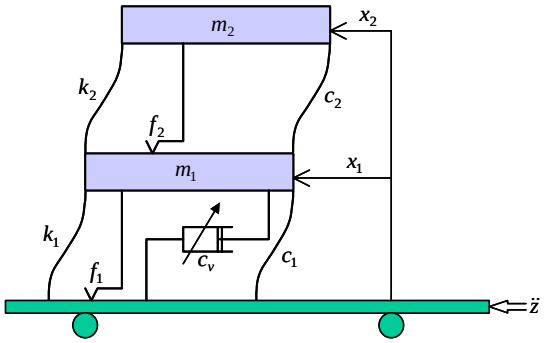

(c) Numerical model

Fig. 1 Experimental Setup and Numerical Model of Specimen

2.1.2 Frequency responses

Fig. 2 shows the frequency responses of first and second story acceleration to the ground acceleration for the numerical model of structure. The first mode is at 0.36Hz (2.8sec) and the second mode is at 1.07Hz (0.94sec) respectively.

2.2 MR Damper Device

2.2.1 Mechanism

Table 1 System Parameters

Parameter		Value
Mass	m_1	5 655.1 [kg]
	m_2	8 770.4 [kg]
Stiffness	k_1	110 880 [N/m]
	k_2	104 950 [N/m]
Damping	c_1	4 527.1 [N s/m]
	c_2	3 591.9 [N s/m]
Friction Force	f_1	471.2 [N]
	f_2	124.0 [N]

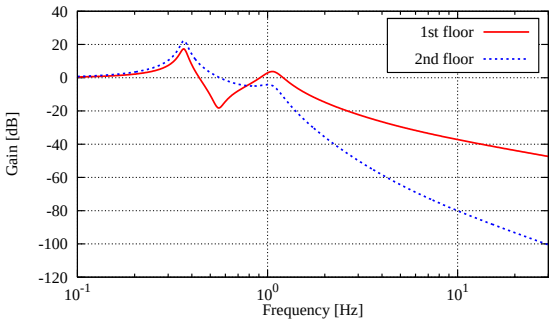

(a) From ground acceleration $\ddot{z}$

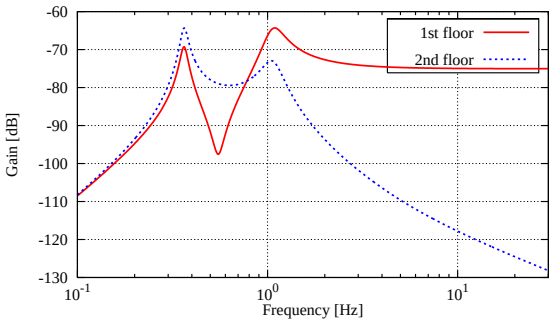

(b) From damping force $u = c_v \dot{x}_1$

Fig. 2 Frequency Responses of Model

The MR damper contains an MR fluid. The principle of this MR damper is simple and similar to oil damper. See Fig. 3. The damper has a piston and a cylinder filled with MR fluid. The flow of the MR fluid generated by piston movement should be lead into the bypass, which difference from some commercial products of MR damper devices [3], and is subjected to magnetic field formed from surrounding coils. The main reason to put the bypass outside of the piston and the cylinder is to make a circuit of electromagnet efficiently.

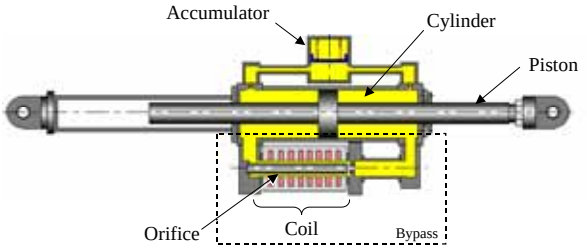

Fig. 3 MR Damper (MRD 40kN-590)

2.2.2 Properties

An MR damper produces variable damping force depending on applied current and stroke velocity of piston movement. Our MR damper has been designed to perform the maximum damping force of 40kN and stroke 295mm for each direction. Therefore, it is very important to set up functions from input current to damping force before applying control.

On Fig. 4, the dashed line shows relations between stroke velocity and damping force at a certain constant current obtained from experimental test. We use the following bilinear model for the MR damper as shown by solid line in Fig. 4.

$$F = \begin{cases} \mathrm{sgn}(\dot{x}) \cdot (0.07 \mid \dot{x}_1 \mid + a(i)) & (\mid \dot{x}_1 \mid \geq 0.1) \\ b(i)\, \dot{x}_1 & (\mid \dot{x}_1 \mid < 0.1) \end{cases} \quad (1)$$

Both $a(i)$ and $b(i)$ in Eq.(1) are assumed as quadric functions about input current i. See Eq.(2) and Fig. 5.

$$a(i) = \hat{a}_1 i^2 + \hat{b}_1 i + \hat{c}_1, \quad b(i) = \hat{a}_2 i^2 + \hat{b}_2 i + \hat{c}_2 \quad (2)$$

where $\hat{a}_1 = 1.5$, $\hat{b}_1 = 2.27$, $\hat{c}_1 = 0.528$, $\hat{a}_2 = 20$, $\hat{b}_2 = 20$ and $\hat{c}_2 = 5.352$ respectively.

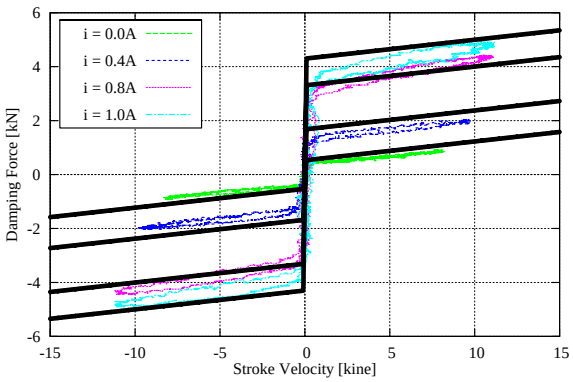

Fig. 4 Characteristics of MR Damper

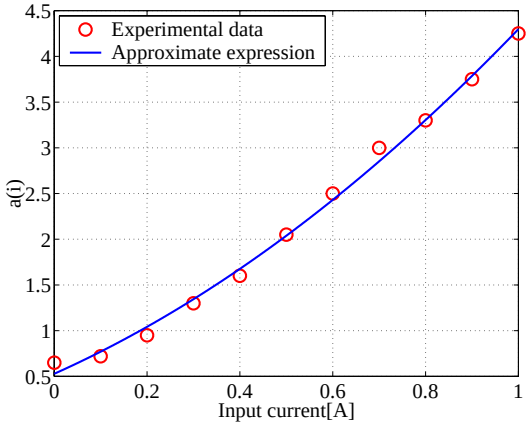

(a) $a(i)$

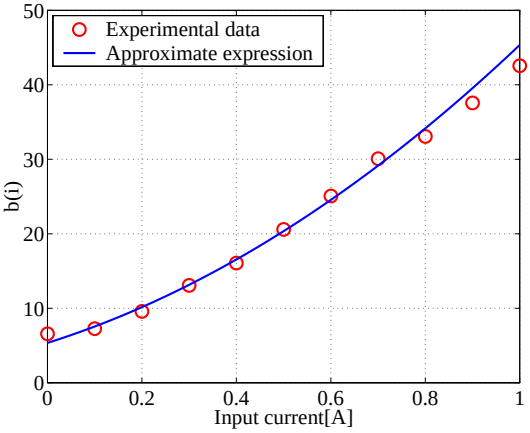

(b) $b(i)$

Fig. 5 Approximation of $a(i)$ and $b(i)$

3. CONTROL SYSTEM DESIGN

3.1 Gain-Scheduled Control Method

We apply a gain-scheduled (GS) control method to calculate an appropriate damping coefficient. The design of the GS controller is based on linear matrix inequalities (LMIs) and the controller is obtained by the convex interpolation of four-vertex linear time-invariant (LTI) controllers [4]. It is well known that the system with a semi-active damper can be modeled as a bilinear system where the input term is linear to both the damping coefficient that is regarded as the control input and the relative velocity. If linear control theory is applied to the bilinear system, switching of damping coefficient should be required frequently and the generated force is not smooth. By assuming a semi-active damper model with a controllable valve the system can be described

as a linear parameter-varying (LPV) model. The LTI controller according to the vertexes can be obtained by applying LMIs and the GS controller is obtained by convex interpolation of the LTI controllers. In this paper we take two varying parameters p_1 of the stroke velocity and p_2 of the damping coefficient restriction. In order to prevent the uncontrollability caused when the stroke velocity is equal to zero, the parameter varying range is divided into two areas around small value of the velocity. See Fig. 6. If parameter is in the range from -0.005 to 0.005, we make the input e zero.

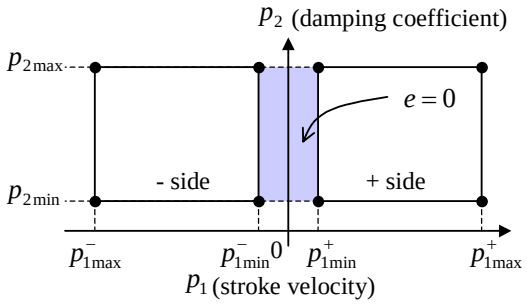

Fig. 6 Separation of Parameter-varying Range

3.2 Weighting Functions

We apply the H-infinity norm criterion for each vertex. The schematic diagram of generalized plant is shown in Fig. 7. While the weighting function W_T is defined not to increase the effect of control force in higher frequency, W_{S1} and W_{S2} cover the first and second mode of the controlled object respectively for reduction of the acceleration response. See Fig. 8. W_T, W_{S1} and W_{S2} are given by eqs. (3), (4) and (5) respectively. Fig. 9 shows the gain of frequency response functions of the controllers at each vertex.

$$W_T = 0.52 \times \frac{s^2 + 2 \cdot 0.8 \cdot (20 \cdot 2\pi) \cdot s + (20 \cdot 2\pi)^2}{s^2 + 2 \cdot 0.4 \cdot (500 \cdot 2\pi) \cdot s + (500 \cdot 2\pi)^2} \tag{3}$$

$$W_{S1} = (8.0 \cdot 2\pi)^{12} \cdot 2.7 \cdot 10^{-14} \times \frac{s^2 + 2 \cdot 0.5 \cdot (0.8 \cdot 2\pi) \cdot s + (0.8 \cdot 2\pi)^2}{s^2 + 2 \cdot 0.5 \cdot (1.0 \cdot 2\pi) \cdot s + (1.0 \cdot 2\pi)^2} \times \frac{1}{(s^2 + 2 \cdot 0.63 \cdot (8.0 \cdot 2\pi) \cdot s + (8.0 \cdot 2\pi)^2)^2} \tag{4}$$

$$W_{S2} = (0.4 \cdot 2\pi)^8 \cdot 0.14^2 \times \frac{1}{(s^2 + 2 \cdot 0.5 \cdot (0.4 \cdot 2\pi) \cdot s + (0.4 \cdot 2\pi)^2)^2} \tag{5}$$

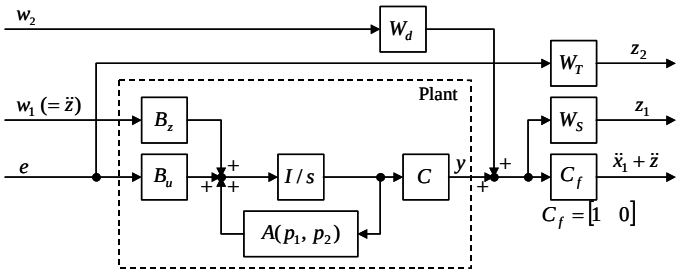

Fig. 7 Generalized Plant

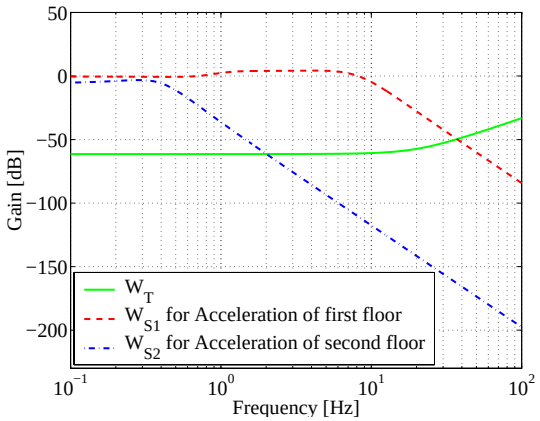

Fig. 8 Weighting Functions

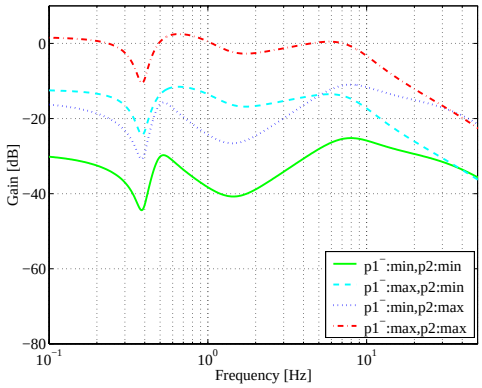

(a) Negative side

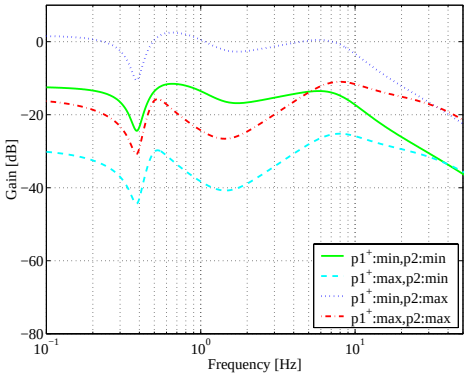

(b) Positive side

Fig. 9 Vertex Controllers

4. RESULTS

4.1 Shaking Table Test

In this section, the performance of the GS controller is compared to the other result of the passive systems with constant damping coefficient 42500 Ns/m, 7000 Ns/m and 24750 Ns/m (mean of former two values) which are referred to as hard, soft and medium damping respectively.

Fig. 10 shows the frequency response of mass acceleration to ground acceleration with the MR damper. From this figure, we can see that not only the first and second modes are suppressed but also the response in higher frequency range than the second mode is suppressed less than a medium damper.

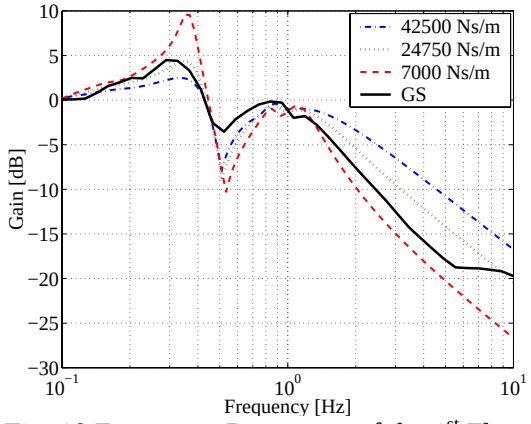

Fig. 10 Frequency Responses of the 1st Floor

Fig. 11 shows the comparison of experimental and analytical results for GS control under Hachinohe 1968NS earthquake normalized as maximum velocity of 25kine. The structural responses of simulation results show good agreement with those of experimental ones except some negligible errors around origin.

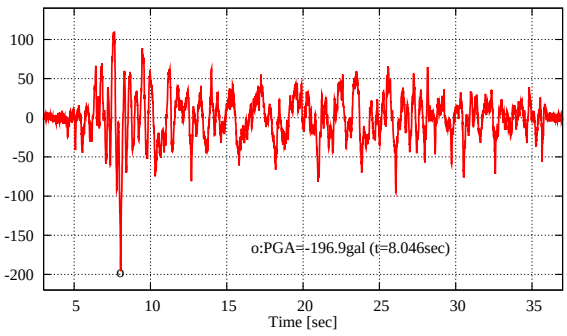

(a) Hachinohe 1968NS earthquake

Fig. 11 Comparison with Analysis (continued)

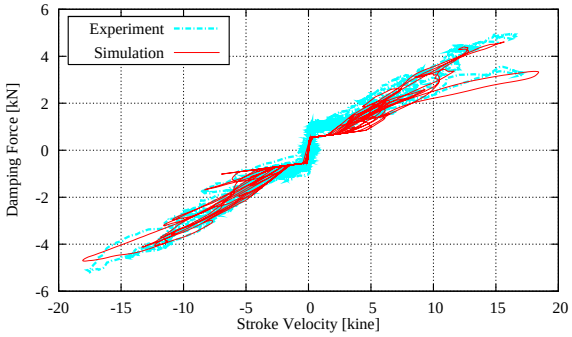

(b) Stroke velocity and damping force

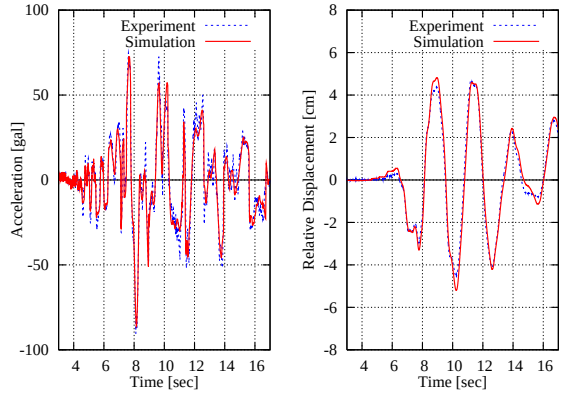

(c) Time history of first floor

Fig. 11 Comparison with Analysis

Fig. 12 (on next page) shows the acceleration response under the GS control in comparison with the passive systems. From Figs. 12(b) and 12(c), it can be seen that the GS controller suppress responses both around the first shock (t=8sec) with small damping coefficient c_v and trailing responses around t=20sec with large c_v like the system with medium damping. From viewpoint of acceleration response the medium passive damper seems better but the GS control system can suppress displacement at the same time. See Fig. 13.

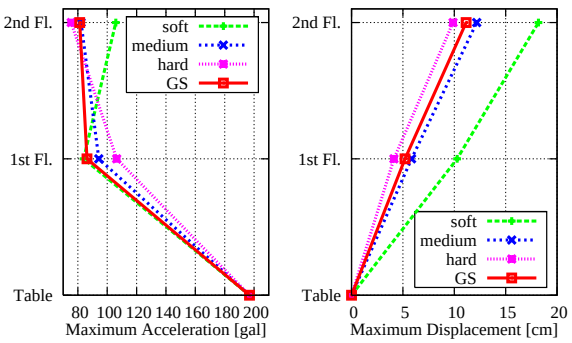

Fig. 13 Maximum Amplitude of Each Floor

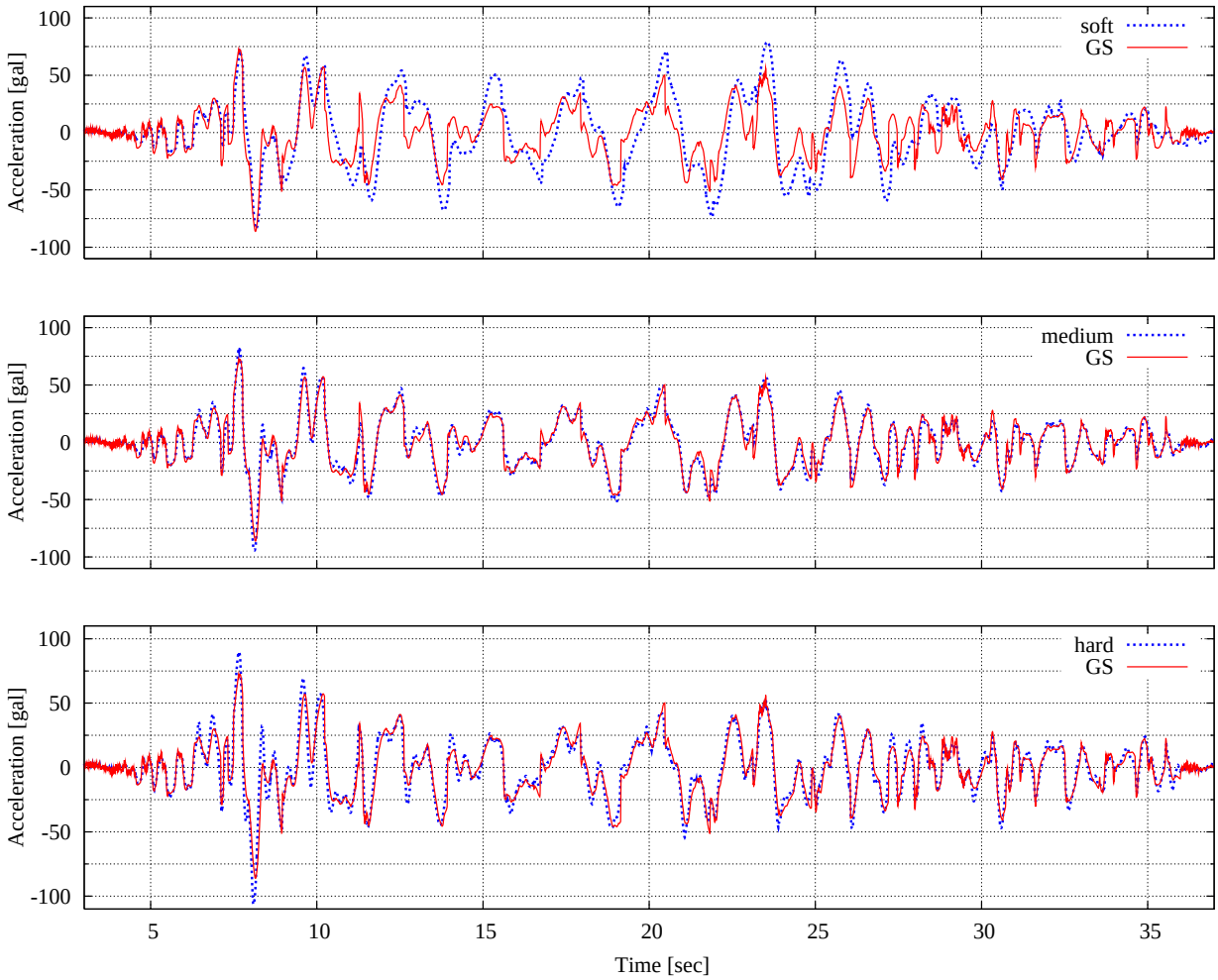

(a) Acceleration of first floor

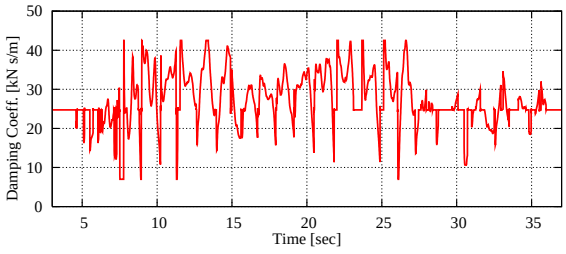

(b) Damping coefficient

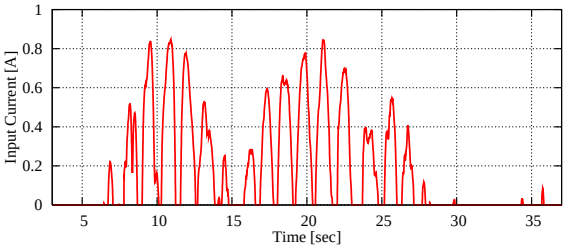

(c) Input current

Fig. 12 Time History of Response

4.2 Performance

It is important to consider not only the time history but also the total input energy to the upper structure. In this section we compare the performance of the GS controller using energy spectrum V_E [5]. The V_E is calculated via eq.(6) for certain SDOF systems with period T and damping factor h under specific inputs.

$$V_E = \int M\ddot{x}\dot{x}\,dx + \int C\dot{x}^2\,dx + \int Kx\dot{x}\,dx \qquad (6)$$

Fig. 14 shows an example result of V_E for the system with damping factor $h = 10\%$ under some inputs held on Table 2. Fig. 14 means the "source" input energy for the structure fixed to the ground. In our case upper structure is settled on the isolation layer, then, the amplification factor from Fig. 14 to the V_E s for the response

of first floor under each input motions can be treated as the performance of isolation.

Fig. 15 shows the amplification factor P for the Hachinohe input motion in Fig. 11(a). The soft damping system has good performance (smaller P) in shorter period (around the second mode T=0.94sec) but got worse in longer period (around the first mode T=2.8sec). Performance of the hard damping system is contrary to that of the soft damping system.

Table 2 Input Motions

Earthquake	Level (Max. Vel.)
Hachinohe 1968 NS	25kine, 50kine
JMA Kobe 1995 NS	25kine, 50kine
El Centro 1940 NS	25kine, 50kine
Taft 1952 EW	25kine

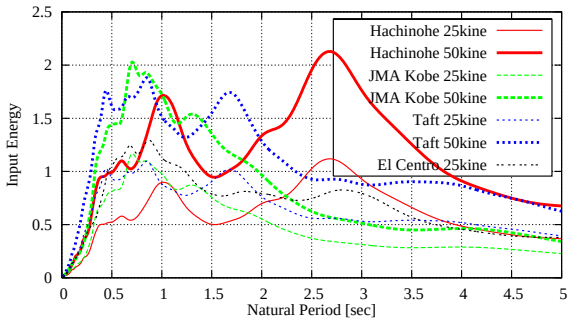

Fig. 14 V_E spectrum ($h = 10\%$)

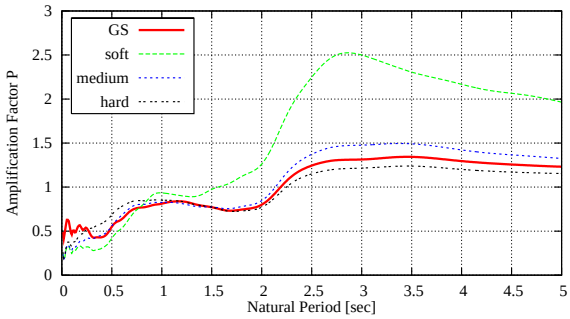

Fig. 15 Comparison of P (Hachinohe 25kine)

Fig. 16 shows average and standard deviation of the value P for seven input motions on Table 2. In Figs. 16(b), 16(c) and 16(d) the average of GS control are plotted together for comparison. It can be seen that there are trade-offs between the response in shorter and longer period. The medium passive damping system shows good performance both in shorter and longer period but the standard deviation of amplitude is worse in longer period compared to the GS controlled system. It can be said that the GS control shows the best performance under various input motions.

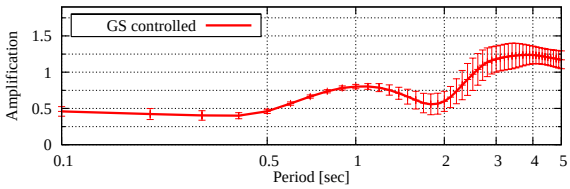

(a) GS control

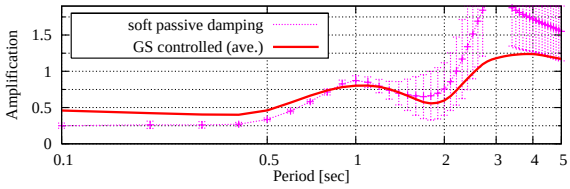

(b) soft damping

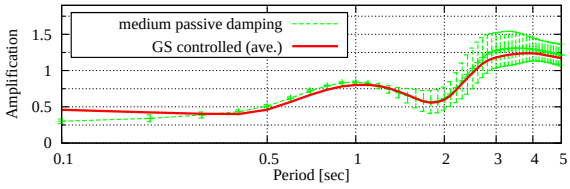

(c) medium damping

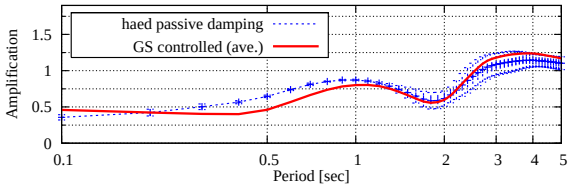

(d) hard damping

Fig. 16 Comparison of P with pasv. systems

5. CONCLUSIONS

A shaking table test and a numerical analysis have been carried out to confirm the efficiency of the semi-active MR damper device for the response control of the base isolated structure.

- The system with the MR damper was properly modeled as an LPV system and the GS control shows higher performance compared to the passive control.
- With the semi-active GS control, both response displacement and acceleration can be suppressed at the same time.
- Input energy for upper structure decreases through wide frequency range.

6. APPENDIX

As mentioned in the above discussion, we take the GS control method based on the H-infinity norm criterion. This control theory focuses on the frequency response through an observation with weighting functions then the two different objectives, response reduction of both isolation layer (at lower period) and upper structure (at higher period), can be performed at the same time with only one damper installed at the isolation layer.

Fig. 17 shows the example result for a 12-story base isolated structure under El Centro 1940 NS (50kine) and Taft 1952 EW (50kine) input motions. For both cases the maximum displacement has most decreased with passive damping but higher mode acceleration response increases while the GS controller can suppress those.

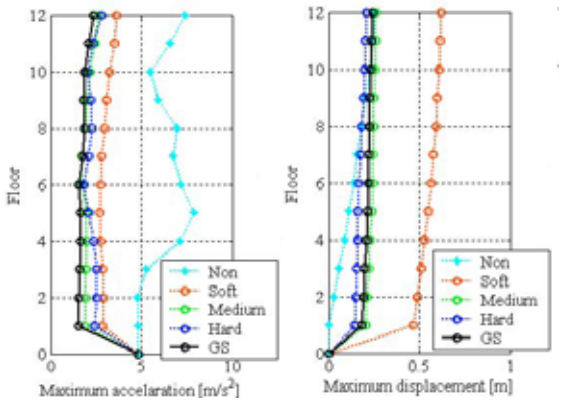

(a) El Centro 1940 NS (50kine)

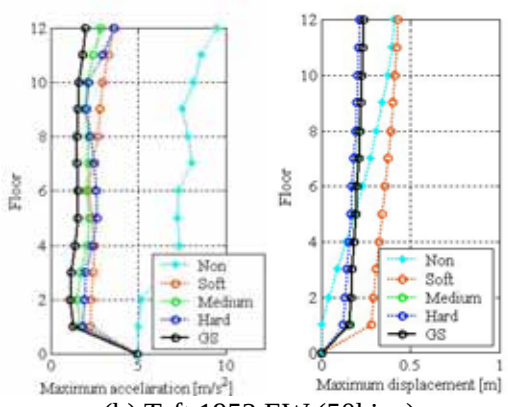

(b) Taft 1952 EW (50kine)

Fig. 17 Result of 12-story Structure

7. ACKNOWLEDGEMENT

A part of this study was financially supported by the Budget for Nuclear Research of the Ministry of Education, Culture, Sports, Science and Technology, based on the screening and counseling by the Atomic Energy Commission.

8. REFERENCES

1. Soda, S., Kusumoto, H., Chatani, R., Iwata, N., Fujitani, H., Shiozaki, Y. and Hiwatashi, T. "Semi-active Seismic Response Control of Base-isolated Building with MR Damper", Proceedings of the SPIE's 10th Annual International Symposium on Smart Structures and Materials, No.5052-56, 2003.
2. Hiwatashi, T., Shiozaki, Y., Minowa, C. and Soda, S. "Shaking Table Tests on Semi-active Base-isolation System by Magnetorheological Fluid Damper", Proceedings of the SPIE's 10th Annual International Symposium on Smart Structures and Materials, No.5056-50, 2003.
3. http://www.lord.com/
4. Nishimura, H., Okumura, Y. and Shimodaira, S. "Semi-active Vibration Isolation Control for Multi-degree-of-freedom Structures", Proc. of 2002 ASME PRESSURE VESSELS & PIPING CONFERENCE, Vol. 445-2, pp.189-196, 2002.
5. Akiyama, H. "Earthquake-Resistant Design Method for Buildings Based on Energy Balance", Gihodo Shuppan Co. Ltd., 1999 (in Japanese).